



ELSEVIER

Available online at www.sciencedirect.com

SCIENCE @ DIRECT®

Journal of Nuclear Materials 319 (2003) 81–86

journal of
nuclear
materialswww.elsevier.com/locate/jnucmat

Irradiation effects on yttria-stabilized zirconia irradiated with neon ions

T. Hojo^a, J. Aihara^{b,*}, K. Hojou^b, S. Furuno^b, H. Yamamoto^b,
N. Nitani^c, T. Yamashita^c, K. Minato^c, T. Sakuma^a

^a Graduate School of Science and Engineering, Ibaraki University, Mito-shi 2-1-1, Ibaraki 310-8512, Japan

^b Department of Materials Science, Japan Atomic Energy Research Institute, Tokai-mura, Ibaraki 319-1195, Japan

^c Department of Nuclear Energy System, Japan Atomic Energy Research Institute, Tokai-mura, Ibaraki 319-1195, Japan

Abstract

In situ TEM observation was performed on yttria-stabilized zirconia during 30 keV Ne⁺ ion irradiation at room temperature, 923 and 1473 K, respectively, and annealing was performed after irradiation. The observed results revealed clear difference in morphology of damage evolution depending on irradiation temperature. In the irradiation at room temperature defect clusters and bubbles were formed homogeneously at random, and defect clusters were formed earlier than bubbles. In the irradiation at 923 K bubbles and dislocation loops are formed heterogeneously almost at the same time. Moreover, bubbles existed almost only on the loop planes but were almost invisible outside of loop planes in the early stage of irradiation. In the irradiation at 1473 K only bubbles were formed and they grew remarkably with the increasing ion fluence. In annealing remarkable growth of bubbles were observed when temperature was raised from 1373 to 1473 K.

© 2003 Elsevier Science B.V. All rights reserved.

1. Introduction

As safe disposal of surplus plutonium from light water reactors and nuclear weapons, burning plutonium as rock-like fuels in light water reactors has been proposed [1–3]. These fuels are planned to be composed of the inert matrix materials such as yttria (Y₂O₃) stabilized zirconia (ZrO₂) (stabilized zirconia for short), spinel, alumina, composite materials made of these ceramics and plutonium. The rock-like fuels should be designed to satisfy the requirement of a chemical stability and a high resistance to radiation damage over a wide temperature range and under severe irradiation conditions.

Stabilized zirconia is considered as principal candidate materials because of their high radiation stability. No amorphization was observed in stabilized zirconia under neutron or ion irradiation to a high damage level

[4–7]. Furthermore, even under conditions such as 1.5 MeV Xe ion irradiation at low temperature (20 K), no amorphization was obtained [8]. These results indicate that stabilized zirconia has strong resistance for irradiation. Concerning the volume swelling, stabilized zirconia showed negligible swelling under fast neutron irradiation [9,10]. On the other hand, volume swelling due to bubble formation under He or Xe ion irradiations in a transmission electron microscope (TEM) was reported to be 1% and 4% for the highest doses applied at 923 and 1473 K, respectively [6]. Very limited information is available, however, for swelling of stabilized zirconia due to ion irradiation. These studies focused on studies of irradiation by neutrons, light ions (e.g. He), or heavy ions (e.g. Xe). Nothing is known, however, for studies of irradiation with ions with medium weight, while fission products are in wide range of atomic mass. Therefore, studies of irradiation with ions with medium weight are interesting from the fundamental viewpoints.

In this study, 30 keV Ne⁺ ions were used. Energy of ions was adjusted to stop large part of implanted ions within specimen with the thickness of several tens nm

* Corresponding author. Tel.: +81-29 282 6360; fax: +81-29 282 6716.

E-mail address: aihara@sspl.tokai.jaeri.go.jp (J. Aihara).

which is typical thickness for TEM observation. Displacement damage also occurs within this thickness. That is, the aim of this study is to observe efficient damage evolution with synergistic irradiation effects under the condition where implanted atoms and formed point defects such as interstitials and vacancies exist together. To clarify the effects of irradiation temperature stabilized zirconia were irradiated at room temperature, 923 and 1473 K, respectively. Some specimens were annealed up to 1473 K after irradiation to examine annealing effects.

2. Experiments

Yttria-stabilized cubic zirconia specimens containing 21 mol% of yttria were used in this study. The specimens suitable for TEM observation were prepared as follows. Disks with 3 mm diameter were cut off from wafers of 0.2 mm thickness using ultrasonic cutter. Such disks were then dimpled in the center part to the thickness of 30 μm . Perforation was achieved in the center part of disks by 5 keV Ar^+ ion milling with an incident angle of 20° to the surface of disks. Final thinning was performed with 2 keV Ar^+ ions at an incident angle of 15° . All thinning was done at ambient temperature. Ion thinned disks were annealed at 1573 K for 5 h in air.

Irradiations and in situ observations were performed in a JEM-2000F TEM coupled directly to a 40 kV ion accelerator. In this instrument ion beam was incident to the specimen surface at an angle of 60° . Irradiating ions were 30 keV Ne^+ ions, which were selected by using a mass-selecting magnet at an ion flux of $5 \times 10^{13} \text{ cm}^{-2} \text{ s}^{-1}$. Irradiations were performed at room temperature, 923 and 1473 K, respectively and all the irradiations were carried out for 10 min, which resulted in a total ion fluence of $3 \times 10^{16} \text{ cm}^{-2}$. For these irradiation conditions, the average range and depth of peak dpa of 30 keV Ne^+ ions were estimated to be 29 and 20 nm, respectively

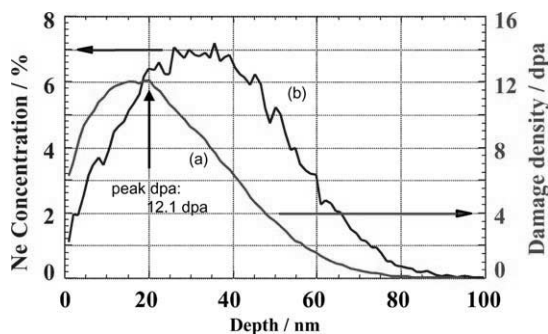


Fig. 1. Distribution of dpa and implanted ions in stabilized zirconia irradiated with 30 keV Ne^+ ions to a fluence of $3 \times 10^{16} \text{ cm}^{-2}$. Calculation was performed by TRIM-code. (a) Damage density due to Ne ion. (b) Depth distribution of Ne atoms.

tively by TRIM calculation [11], using a calculation density of 5.48 g cm^{-3} . The calculated results are shown in Fig. 1. In the case of the specimens irradiated with Ne ions at room temperature and 923 K, these were annealed in the TEM after ion irradiations to understand the annealing behavior. Temperature was raised stepwise at 100 K intervals from 1073 to 1473 K in a Gatan single tilting heating stage. At each annealing stage specimens were kept in constant temperature for 10 min. Excess time for taking photos and raising temperature was several minutes.

3. Results

3.1. Damage evolution by 30 keV Ne^+ ion irradiation

Fig. 2 shows sequential electron micrographs of damage evolution in stabilized zirconia irradiated with 30 keV Ne^+ ions with an ion flux of $5 \times 10^{13} \text{ cm}^{-2} \text{ s}^{-1}$ at room temperature. Tiny defect clusters were observed as dot contrast at an ion fluence of $1.5 \times 10^{15} \text{ cm}^{-2}$, as shown in Fig. 2(a). Its size increased gradually with the increasing fluence and turned to dislocation loops after the ion fluence of $6 \times 10^{15} \text{ cm}^{-2}$. Dislocation loops overlapped and tangled after the ion fluence of $1.5 \times 10^{16} \text{ cm}^{-2}$. Bubbles were observed at an ion fluence of $6 \times 10^{15} \text{ cm}^{-2}$, as shown in Fig. 2(c). The bubbles grew further to an ion fluence of $3 \times 10^{16} \text{ cm}^{-2}$. Their diameters were 1.5 nm at maximum. In the specimen irradiated at room temperature bubbles were formed later than dislocation loops. No amorphization was observed under this condition.

Fig. 3 shows sequential electron micrographs of damage evolution in stabilized zirconia irradiated with 30 keV Ne^+ ions at 923 K. Dislocation loops were formed within the ion fluence of $3 \times 10^{15} \text{ cm}^{-2}$, as shown in Fig. 3(a) and its growth speed was much higher than that irradiated at room temperature. Loops tangled soon with each other at $6 \times 10^{15} \text{ cm}^{-2}$. Interesting structure of loops was found by detailed inspection of Fig. 3(a). Tiny bubbles existed only on the loop planes but were almost invisible outside of loop planes at the ion fluence of $3 \times 10^{15} \text{ cm}^{-2}$, that is, bubbles were formed heterogeneously in the early stage of irradiation at this temperature. Bubbles were formed in the whole region at the ion fluence of $6 \times 10^{15} \text{ cm}^{-2}$, as shown in Fig. 3(b). Bubble size increased with the increasing fluence. Their diameter reached 3 nm at maximum at an ion fluence of $3 \times 10^{16} \text{ cm}^{-2}$. In the specimen irradiated at 923 K dislocation loops and bubbles were observed to be formed almost at the same time at an early stage of $3 \times 10^{15} \text{ cm}^{-2}$, as shown in Fig. 3(a).

Fig. 4 shows sequential electron micrographs of damage evolution in stabilized zirconia irradiated with 30 keV Ne^+ ions at 1473 K. Bubbles were formed at an

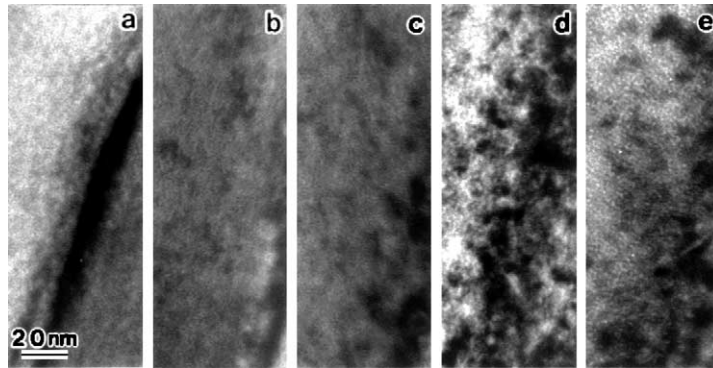


Fig. 2. Sequential electron micrographs showing the damage evolution of stabilized zirconia during irradiation with 30 keV Ne^+ ions of ion flux of $5 \times 10^{13} \text{ cm}^{-2} \text{ s}^{-1}$ at room temperature, for the following fluence: (a) $1.5 \times 10^{15} \text{ cm}^{-2}$, (b) $3 \times 10^{15} \text{ cm}^{-2}$, (c) $6 \times 10^{15} \text{ cm}^{-2}$, (d) $1.5 \times 10^{16} \text{ cm}^{-2}$, (e) $3 \times 10^{16} \text{ cm}^{-2}$.

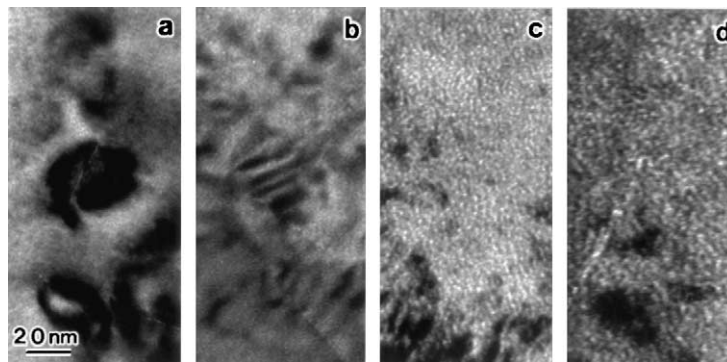


Fig. 3. Sequential electron micrographs showing the damage evolution of stabilized zirconia during irradiation with 30 keV Ne^+ ions of ion flux of $5 \times 10^{13} \text{ cm}^{-2} \text{ s}^{-1}$ at 923 K, for the following fluence: (a) $3 \times 10^{15} \text{ cm}^{-2}$, (b) $6 \times 10^{15} \text{ cm}^{-2}$, (c) $1.5 \times 10^{16} \text{ cm}^{-2}$, (d) $3 \times 10^{16} \text{ cm}^{-2}$.

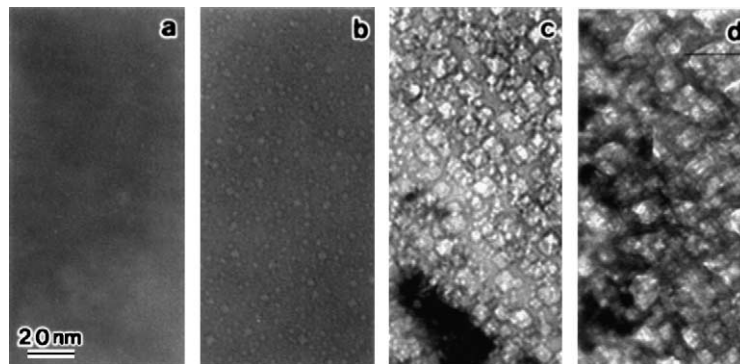


Fig. 4. Sequential electron micrographs showing the damage evolution of stabilized zirconia during irradiation with 30 keV Ne^+ ions of ion flux of $5 \times 10^{13} \text{ cm}^{-2} \text{ s}^{-1}$ at 1473 K, for the following fluence: (a) $3 \times 10^{15} \text{ cm}^{-2}$, (b) $6 \times 10^{15} \text{ cm}^{-2}$, (c) $1.5 \times 10^{16} \text{ cm}^{-2}$, (d) $3 \times 10^{16} \text{ cm}^{-2}$.

ion fluence of $6 \times 10^{15} \text{ cm}^{-2}$, as shown in Fig. 4(b). Bubbles grew with the increasing fluence, while their

density hardly increased. Their diameters reached 13 nm at maximum at the ion fluence of $3 \times 10^{16} \text{ cm}^{-2}$. It is

thought that such large bubbles cause serious swelling. As for dislocation loops, complicated strain contrast accompanied with thickness fringe contrast appeared but these did not lead to stable dislocation loops. In the specimen irradiated at 1473 K bubbles were formed but stable dislocation loops were not formed.

The observed results show clear difference in morphology of damage evolution depending on irradiation temperature of stabilized zirconia irradiated with 30 keV Ne⁺ ions. As for bubbles, the higher irradiation temperature is, the larger bubbles grow.

3.2. Damage evolution during annealing after Ne⁺ ion irradiation

Specimens irradiated with Ne⁺ ions at room temperature or 923 K were annealed up to 1473 K.

Fig. 5 shows damage evolution in stabilized zirconia during annealing after 30 keV Ne⁺ ion irradiation to an ion fluence of $3 \times 10^{16} \text{ cm}^{-2}$ at room temperature. Temperature was raised straightly to 1073 K, and then raised stepwise at 100 K intervals for 10 min from 1073

to 1473 K. Bubbles grew a little, while the temperature was raised from room temperature to 1073 K, as shown in Fig. 5(a) and (b). Then they grew gradually with the increasing annealing temperature to 1373 K. They grew noticeably while the temperature was raised from 1373 to 1473 K.

Fig. 6 shows damage evolution in the specimen during annealing after Ne⁺ ion irradiation at 923 K. The bubble sizes were nearly the same during annealing up to 1073 K after the irradiation at 923 K. Bubbles began to grow gradually with the increasing annealing temperature (1073–1373 K) and grew large by Ostwald ripening or coalescence of bubbles when temperature was raised from 1373 to 1473 K, as shown in Fig. 6(e). When these observed results of specimen annealed up to 1473 K after Ne⁺ ion irradiation at room temperature or 923 K are compared with those of specimens irradiated at 1473 K (Fig. 4(d)), significant differences are seen in the process of bubble growth and its morphology. The higher the irradiation temperature is, the larger bubbles grow, regardless of the careers of irradiation and annealing. Remarkable bubble growth is observed in the

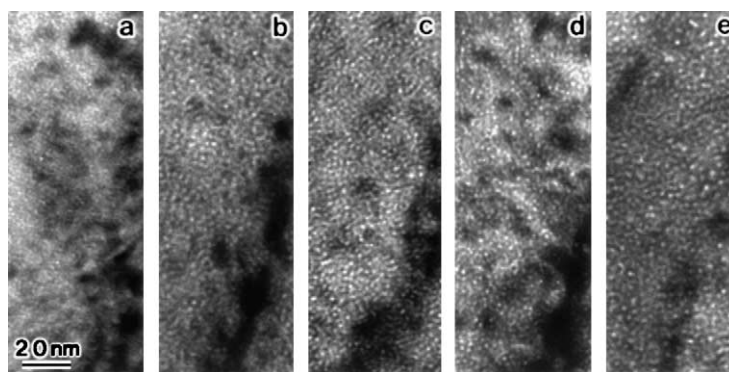


Fig. 5. TEM image of stabilized zirconia during annealing after 30 keV Ne⁺ ion irradiation to an ion fluence of $3 \times 10^{16} \text{ cm}^{-2}$ at room temperature: (a) as irradiated, (b) 1073 K, (c) 1273 K, (d) 1373 K, (e) 1473 K.

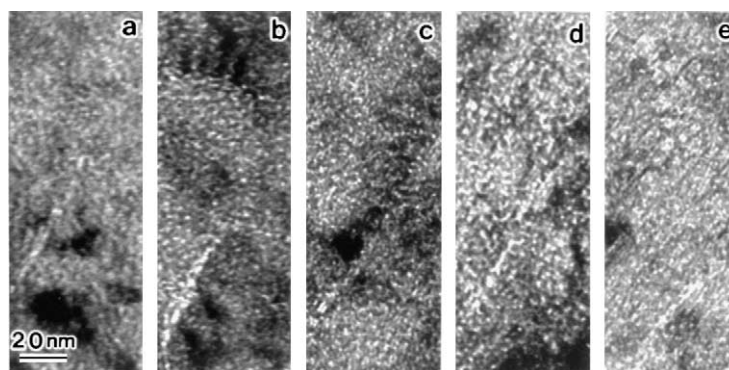


Fig. 6. TEM image of stabilized zirconia during annealing after 30 keV Ne⁺ ion irradiation to an ion fluence of $3 \times 10^{16} \text{ cm}^{-2}$ at 923 K: (a) as irradiated, (b) 1073 K, (c) 1273 K, (d) 1373 K, (e) 1473 K.

specimen irradiated at 1473 K, compared with the specimens annealed up to 1473 K after Ne⁺ ion irradiation at room temperature or 923 K.

4. Discussion

In situ TEM observation of stabilized zirconia during 30 keV Ne⁺ ion irradiation revealed damage evolution behavior characteristic of irradiation temperature.

In the irradiation at low temperature such as room temperature, defect clusters were formed earlier than bubbles in the early stage of irradiation, as shown in Fig. 2(a)–(c). It is thought that mobility of interstitial is much larger than that of vacancy. These interstitials combine and cluster smoothly, and these clusters turn to dislocation loops in early stage of irradiation. Growing dislocation loops act as efficient sinks for interstitials and suppress density of interstitials. Excess vacancies in the vicinity of dislocation loops aggregate easily and lead to bubble formation by trapping gas atoms. At low temperature, however, mobility of point defects such as interstitials is low, compared with that at high temperature. This results in a decrease of growth speed of defect clusters in the irradiation at low temperature. Slowly growing dislocation loops act as weak sinks for interstitials and barely suppress the density of interstitials. In the neighborhood of already formed defect clusters, another defect cluster may be newly formed, resulting in homogeneous formation of defect clusters.

In the irradiation at medium temperature such as 923 K, interesting morphology of damage was observed at early stage of irradiation. By detailed observation, bubbles were observed to exist almost only on the loop planes, but almost invisible outside of loop planes at the irradiation with an ion fluence of $3 \times 10^{15} \text{ cm}^{-2}$, as shown in Fig. 3(a). This implies that bubbles were formed heterogeneously at early stage of irradiation at this temperature. Bubble formation on loop plane had also been found in the case of alumina irradiated with H or He [12,13]. Such bubble formation may be common feature in the ion irradiation at medium temperature. About phenomenon like these, we suppose that bubble formation at early stage of irradiation is promoted by rapid growth of loops, namely, rapid growth of loops absorbs many interstitial atoms. These result in large depression of instantaneous density of interstitials in the vicinity of dislocation line when it is moving. Depression of density of interstitials raises simultaneously relative density of vacancies in the vicinity of dislocation line, which assists formation of bubbles in the periphery of loops at early stage of irradiation. After all, loops leave the formed bubbles inside the loops, because loops extend. Thus, in order that bubble formation are promoted by rapid growth of loops, bubbles are formed earlier at this temperature than at room temperature and

1473 K, as shown from comparison of image in Fig. 3(a) with that in Figs. 2(c) and 4(b). It should be noticed that feature of damage evolution in irradiation at medium temperature can be observed only in the early stage of irradiation. As irradiation proceeds this feature is blurred by growth, overlap and tangle of dislocation loops. After the irradiation proceeds apparent damage morphology in the irradiation at medium temperature resembles that at low temperature, though there is difference in size and density of dislocation loops and bubbles.

At high temperature, such as 1473 K, mobility of interstitials is extremely high so that large part of interstitials may escape to the surface of the thin specimen and the probability of decomposition of defect clusters is high, even if defect clusters are instantaneously formed. Therefore, formation of interstitial loop is considered to be difficult. On the contrary, mobility of vacancies is also high, but is not so high as that of interstitials. Therefore the effect of the surface sink of thin specimen is weak for vacancies, compared with interstitials. Vacancies can be combined with each other by trapping moving implanted Ne atoms, and grow smoothly. Thus bubble formation is preferable to loop formation at high temperature, as shown in Fig. 4.

5. Summary

Results obtained in these studies are summarized as follows.

The case of irradiation with 30 keV Ne⁺ ions

1. In the specimen irradiated at room temperature, defect clusters are formed earlier than bubbles and they formed homogeneously.
2. In the specimen irradiated at 923 K dislocation loops and bubbles are formed almost at the same time. Besides bubbles are formed preferentially on loop plane at early stage of irradiation.
3. In the specimen irradiated at 1473 K growth of bubbles are remarkable, but dislocation loops are not formed.
4. During annealing bubbles grow. Especially growth is remarkable, while temperature rises from 1373 to 1473 K.

References

- [1] H. Akie, T. Muromura, H. Takano, S. Matsuura, Nucl. Technol. 107 (1994) 182.
- [2] N. Nitani, H. Akie, H. Takano, T. Ohmichi, T. Muromura, in: Proceedings of the PSI Workshop on Advanced Fuel Cycle, PSI, Switzerland, 18–19 September 1995, p. 118.

- [3] C. Degueldre, U. Kasemeyer, F. Botta, G. Ledergerber, *Mater. Res. Soc. Symp. Proc.* 412 (1996) 15.
- [4] E.L. Fleischer, M.G. Norton, M.A. Zaleski, W. Hertl, C.B. Carter, J.W. Mayer, *J. Mater. Res.* 6 (1991) 1905.
- [5] N. Yu, K.E. Sickafus, P. Kodali, M. Nastasi, *J. Nucl. Mater.* 244 (1997) 266.
- [6] N. Sasajima, T. Matsui, K. Hojou, S. Furuno, H. Otsu, K. Izui, T. Muromura, *Nucl. Instrum. and Meth. B* 141 (1998) 487.
- [7] K.E. Sickafus, H.J. Matzke, K. Yasuda, P. Choda III, R.A. Verrall, P.G. Lucuta, H.R. Andrew, A. Turos, R. Fromknecht, N.P. Baker, *Nucl. Instrum. and Meth. B* 141 (1998) 358.
- [8] C. Degueldre, P. Heimgartener, G. Ledergerber, N. Sasajima, K. Hojou, T. Muromura, L. Wang, W. Gong, R. Ewing, *Mater. Res. Soc. Symp. Proc.* 439 (1997) 625.
- [9] F.W. Clinard Jr., G.F. Hurley, L.W. Hobbs, *J. Nucl. Mater.* 108&109 (1982) 655.
- [10] F.W. Clinard Jr., D.L. Rohr, W.A. Ranken, *J. Am. Ceram. Soc.* 60 (1977) 287.
- [11] J.F. Ziegler, J.P. Biersack, U. Littmark, *The Stopping and Range of Ions in Solids*, Pergamon, New York, 1985.
- [12] S. Furuno, N. Sasajima, K. Hojou, K. Izui, H. Otsu, T. Matsui, *J. Nucl. Mater.* 258–263 (1998) 1817.
- [13] N. Sasajima, T. Matsui, S. Furuno, K. Hojou, H. Otsu, *Nucl. Instrum. and Meth. B* 148 (1999) 745.